Suppression of Superfluidity of ^{3}He in Cylindrical Channels

V. Kotsubo,[(1),(2)] K. D. Hahn,[(1)] and J. M. Parpia[(1),(2)]

[(1)]*Physics Department, Texas A & M University, College Station, Texas 77843*

[(2)]*Laboratory of Atomic and Solid State Physics, Cornell University, Ithaca, New York 14853*

(Received 12 September 1986)

We have measured the suppression of superfluidity of liquid ^{3}He in small cylindrical pores. The suppression is smaller than calculated by recent theories, and indicates that a dissipative state intervenes before true superflow through the pores commences. The critical currents are 2 orders of magnitude lower than those measured in the bulk, and do not show the same power-law behavior.

PACS numbers: 67.50.Fi, 67.40.Hf

The boundary condition on the order parameter of superfluid ^{3}He results in a suppression of at least one component of the three-dimensional order parameter near a surface. The influence of the surface should extend over a distance of several coherence lengths,[1] and in long cylindrical pores, the constraints imposed by the confining geometry could produce other than the usual A or B phases observed in bulk liquid.[2] These boundary effects are strongly dependent on whether the surface is diffuse or specular to incident quasiparticles.[3] For pores with radii on the order of the zero-temperature coherence length, the superfluid density and the transition temperature should be suppressed[4] since the coherence length diverges at the bulk transition temperature. Another result should be a low critical velocity due to a suppressed gap.

It was with the aim of exploring these effects that we undertook this experiment. ^{3}He is particularly well suited for this investigation since the zero-temperature coherence length, $\xi_0 = \hbar v_F/2\pi k_B T_c$, is strongly pressure dependent, varying from about 700 Å at low pressures to about 150 Å at melting pressure. Thus, in a particular experimental configuration, by adjusting the pressure, the ratio of coherence length to cell dimension can be varied by a factor of 5.

Nuclepore filter,[5] of nominal size 4000 Å, was selected as the confining geometry since this material has straight pores of relatively uniform size. An examination of electron micrographs by the manufacturer and by us showed a pore size of 3500 ± 200 Å and a porosity of 12.6%. Photographs of a random 20-μm^2 area revealed several clusters where two or more pores overlapped at the surface. However, within these large "holes," tracks corresponding to single pores were imaged. Evidently the majority of pores are not perpendicular to the surface. Therefore, the likelihood of two overlapping pores being parallel is exceedingly small. Finally, there is evidence[6] that the pore cross section may be barrel shaped. Nuclepore filter has been used in a previous experiment by Manninen and Pekola,[7] in which critical currents were studied. Packed powders[8] or fibrous materials have broad size distributions and poorly defined geometries and thus were not suitable for this experiment.

The experimental cell is illustrated in Fig. 1. An annular flow channel, with dimensions 0.25 mm width $\times$ 1.25 mm height, was built on a 7.6-mm radius. The Nuclepore filter was glued into a pair of frames and then inserted across the channel. The flow cell was mounted on a torsion tube and formed an oscillator with a resonant frequency of about 850 Hz.

This arrangement functions as a highly sensitive detector of superfluidity of ^{3}He in the pores through the measurement of the period of the oscillator. When the fluid in the pores is normal, the membrane presents a high flow impedance to the fraction of fluid in the channel not locked by viscosity. In this case, the entire fluid mass is strongly coupled to the oscillator. When the ^{3}He in the pores is in the superfluid state, the impedance of the membrane becomes negligible, allowing the superfluid mass in the annulus to decouple and lower the period of the oscillator. In principle, this technique would produce

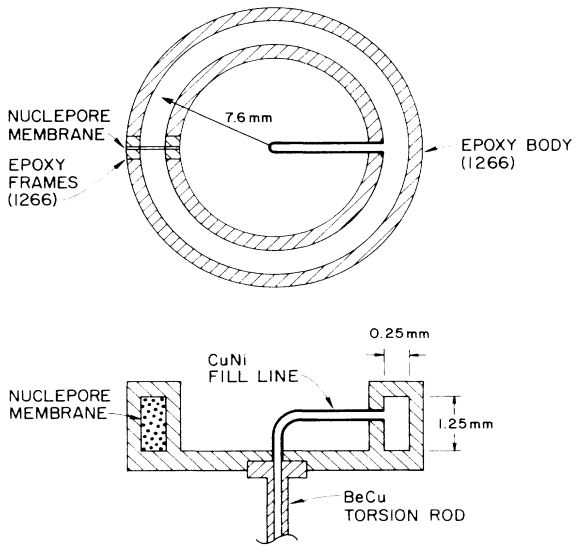

FIG. 1. A schematic view of the experimental cell showing the dimensions.

an abrupt decrease in the period of the oscillator with the onset of superflow. In practice, the transition region is characterized by a finite width which depends on the impressed oscillation amplitude. Our ac technique has the ability to produce low flow velocities, and has high sensitivity to pressure differences across the membrane.[9]

In the limit of incompressibility and complete viscous locking of the normal fluid, two equations describe the hydrodynamics. First, in the rest frame of the laboratory, the conservation of circulation can be written

$$v_s 2\pi R + v_p l = 0. \quad (1)$$

Here, v_s is the superfluid velocity in the channel, v_p is the superfluid velocity in the pores, R is the radius of the annulus, and l is the thickness of the membrane. If we define χ as the fraction of superfluid that is coupled to the oscillator, then v_s is related to v_m, the velocity of the membrane, by $v_s = \chi v_m$. The amount of fluid that is decoupled from the oscillator must backflow through the orifice, so that conservation of mass gives

$$-(1-\chi) v_m A \rho_{sb} = v_p A P \rho_{sp}, \quad (2)$$

where ρ_{sb} is the bulk superfluid density, ρ_{sp} is the superfluid density in the pores, A is the area of the channel, and P is the porosity of the membrane. Combining these two equations determines χ:

$$\chi/(1-\chi) = (l/2\pi RP)\rho_{sb}/\rho_{sp}. \quad (3)$$

By substituting the geometrical factors from our experimental configuration, we find that as long as the superfluid density in the pore is reduced by no less than a factor of 10^2 below that in the bulk, χ is very close to zero. In other words, when even a weakly developed superfluid state exists in the pores, the inertia due to the Kelvin drag of the membrane is small compared to the inertia of the rest of the fluid so that the oscillator behaves as though the membrane were not present.

Experiments were carried out by our cooling the liquid to a temperature on the order of $0.7T/T_c$ or below, and operating the oscillator in a phase-locked loop to track the resonant frequency. The amplitude of oscillation was maintained at a constant level from as low as ~ 0.5 Å peak to peak at all pressures to in excess of 50 Å at low pressures. The cell was then warmed through the transition region at about 15–20 μK/h. At this rate, no thermal offset was observed between the thermometer and the experiment. The period and dissipation of the oscillator were recorded, together with the out-of-balance signal from a lanthanum-doped cerium magnesium nitrate thermometer. Upon warming through the bulk transition temperature, the cell was cooled through the same temperature range at a different amplitude and the procedure repeated. An entire sequence at a single amplitude took approximately 20 h to complete.

A representative set of data is shown in Fig. 2. Here the period of the oscillator is plotted against temperature

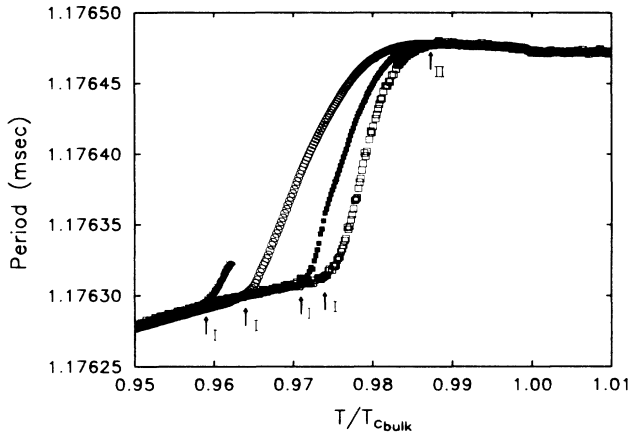

FIG. 2. Results of four runs at different amplitudes 0.61 Å (open squares), 1.9 Å (filled squares), 6.1 Å (open circles), and 9.1 Å (filled circles) at a pressure of 20 bars. We plot the period of the oscillator against the temperature. Features to note are the signature at the bulk transition at ~ 2.445 mK, feature II which marks the onset of superfluidity in the pores, and feature I the onset of dissipative superflow for a particular amplitude.

for four different amplitudes of oscillation. The period shift shows several different features which are noteworthy. As the cell is cooled, the onset of superfluidity in the bulk annular region is marked by a small abrupt rise in the period of the oscillator. This feature is amplitude independent and is thought to be produced by a fourth-sound mode in the channel driven off resonance. At lower temperatures, the period shift becomes amplitude dependent, and at still lower temperatures the data once again become independent of amplitude with the data at various amplitudes all collapsing onto a single universal curve.

Our interpretation of these curves is simple. For any given amplitude, below a certain temperature, labeled I, the liquid in the pores is in the superfluid state and is below its critical current. It thus presents no flow restriction to the rest of the fluid in the channel. Above that particular temperature, the period increases as a result of a finite pressure difference across the pores which accelerates the superfluid in the annular region. This pressure difference is an indication that velocity-induced dissipative flow is occurring in the channels. Thus, for a particular induced velocity through the channels, the membrane's impedance is observed to increase dramatically as the cell is warmed above a certain temperature. At temperatures above feature I, the data do not fall onto a universal curve until a certain temperature, labeled II, is reached. This feature is universal for all amplitudes, and we associate this point with the onset of superfluidity in the pores. Through the conservation of mass [Eq. (2)], J_s, the current flowing through the membrane, is given by $(1-\chi) v_m \rho_{sb}/P$. With use of the usual

temperature dependence of the superfluid density[10] and the assumption that $\chi \simeq 0$, the superfluid current backflowing through the pores can be inferred. The assumption that χ does not differ appreciably from zero should only introduce a significant error close to the transition.

Following the theoretical work of Vollhardt, Maki, and Schopohl,[11] who find that the critical current should follow a relation $J_{sc} = A(1 - T/T_c)^{3/2}$, we plot $J_{sc}^{2/3}$ against the reduced temperature in Fig. 3, and determine the temperature for feature I in the limit of zero current. Our results at all pressures are qualitatively similar and do not agree with this power law; rather, the apparent best exponent lies between $\frac{3}{2}$ and 2 for this range of temperatures. It is possible that this effect is due to a size distribution of the pores. In addition, the value of the critical current at a given temperature is between 2 and 3 orders of magnitude smaller than those measured in previous experiments.[7,12-14]. Finally, the limiting temperature of feature I is different from that of feature II (see Fig. 3).

We now compare our results to earlier critical current experiments. Briefly, Eisenstein, Swift, and Packard[12] observed that the saturated critical currents at 0 bar followed the expected $\frac{3}{2}$ power law. Manninen and Pekola,[7] using Nuclepore filter of 8000-Å pore size, observed the same power-law behavior in two regimes. From their data a low-dissipation regime was resolved at pressure differences of < 2 μbar, and a high-dissipation regime was associated with the saturated critical current. Ling, Betts, and Brewer[13] also observed two flow regimes similar to those in Ref. 7, but found, at pressures greater than 21.5 bars, that the power law switched to 2 rather than the $\frac{3}{2}$ seen at low pressures. Finally in a recent experiment, Pekola and co-workers[14] using a single 7000-Å orifice observed the expected $\frac{3}{2}$ power-law behavior at 0 and 2.4 bars, but with some suppression of the saturated critical current over that in the bulk. Over all, the pressure sensitivity of these experiments was in the range of 1 to 10^{-3} μbar, as compared to our value of 10^{-5} μbar. Further, these experiments generally observe the saturated value of the critical current rather than the onset of dissipative flow as shown in Fig. 2. In view of our higher sensitivity to pressure differences, together with the earlier observation of two dissipative states, it is likely that our enhanced resolution permits us to identify a novel, low-dissipation state in ^{3}He-B, which intervenes well before the saturation critical current is achieved. We are unable to drive the flow cell with currents comparable to those in earlier experiments because of the high amplitudes that this would require and consequent heating.

It is unlikely that our observations are due to some inherent defect in the Nuclepore substrate. We emphasize that our Nuclepore samples were not different (except for a factor of 2 smaller in size) from those used in Ref. 7. As evidence for the relatively sharp pore-size distribution, we can point to the narrowness of the onset of disspative flow in Fig. 2. If a few very large pores were present and controlling the flow, then at temperatures sufficiently below T_c in the smaller pores the critical currents should approach the usual saturated values since presumably all pores would be participating in the flow. Clearly, this is not the case since we observe the low critical currents over the entire range of temperatures accessible to our cell.

The results discussed above are typical for the B phase. At 29 and 23.5 bars, we find that feature I is seen

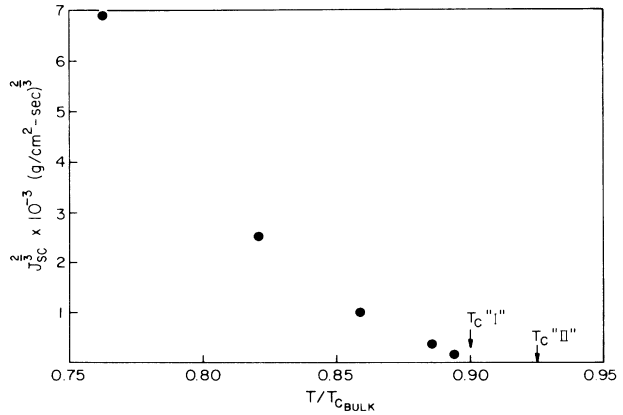

FIG. 3. Critical current, $J_{sc}^{2/3}$, plotted against the reduced temperature for data taken at 1.5 bars. The data are inconsistent with a $\frac{2}{3}$ power law. T_c "I" and T_c "II" mark the temperatures of features I and II, respectively.

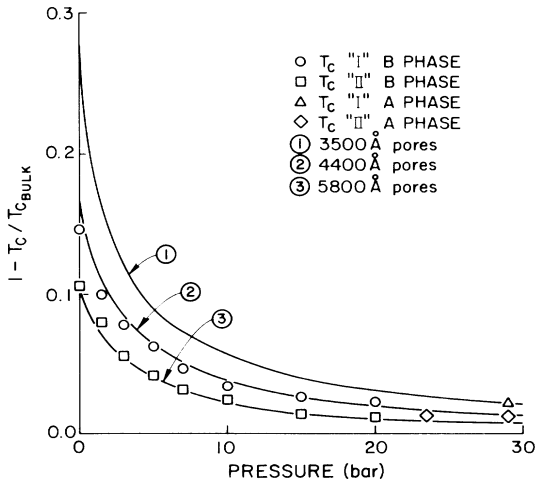

FIG. 4. Pressure dependence of features I and II. Shown for comparison are the result of the calculation of Kjäldman, Kurkijärvi, and Rainer in Ref. 3 (as solid lines), for pore sizes of 3500, 4400, and 5800 Å. Note that the data obtained above the polycritical point show greater suppression than corresponding data in the B phase.

TABLE I. Values of the reduced temperature for features I and II at all pressures.

Pressure (bars)	$T_c(\mathrm{I})/T_{c\,\mathrm{bulk}}$	$T_c(\mathrm{II})/T_{c\,\mathrm{bulk}}$
0	0.853	0.894
1.5	0.900	0.925
3	0.921	0.943
5	0.937	0.957
7	0.952	0.968
10	0.965	0.976
15	0.973	0.986
20	0.976	0.989
23.5	...	0.986
29	0.977	0.989

in the A phase as well, but occurs at lower temperatures than expected by extrapolation of the B-phase results. The critical currents are also lower.

Kjäldman, Kurkijärvi, and Rainer[3] assumed diffuse scattering of quasiparticles, and in the Ginzburg-Landau limit found an expression for the suppression of the transition temperature in terms of the ratio of pore radius to coherence length. A numerical calculation to extend the results to all temperatures was also presented, and because of the large suppression has to be used in comparison to our results for both features I and II which are shown in Fig. 4 and listed in Table I. In addition, we plot in this figure the expected behavior for the 3500-Å pore size together with suppressions calculated for pore sizes of 4400 and 5800 Å, which fit the pressure dependence of features I and II, respectively. If the pores are indeed barrel shaped, our measured suppression of T_c for feature I is within the range of that calculated,[3] but it is unlikely that the pores are distorted to the extent of finding agreement with feature II and the calculations.

Manninen and Pekola[7] found good agreement with the calculations of Kjäldman, Kurkijärvi, and Rainer[3] for the suppression of the transition temperature. The recent results of Pekola[14] show somewhat greater suppression for nearly the same pore size (7000 Å), which they find to be consistent with a model of the polar phase in the pores. Once again, the results are obtained for saturated critical currents rather than the onset of dissipative flow seen in our experiments.

To summarize, we have observed the existence of a novel low-dissipation state in ^{3}He confined within 3500-Å pores. This state is characterized by a critical current 2 to 3 orders of magnitude below the saturated critical currents observed in earlier experiments and exhibits a different temperature dependence. The observation of this state is made possible by our ability to resolve small pressure differences using an ac flow cell. The superfluidity of ^{3}He is suppressed to $0.85T/T_c$ at low pressure but is smaller than expected unless a nonuniform pore cross section is assumed. The mechanism for these effects has not been identified, and it is unclear whether it is induced by the small pore size or by other than bulk order parameters induced by the cylindrical symmetry and flow. We plan to extend our results to smaller pores in the near future.

The authors wish to thank G. Agnolet, W. Saslow, D. Rainer, J. D. Reppy, and R. E. Packard for their comments. This research was supported by the National Science Foundation through Grants No. DMR-8517633 and No. DMR-8218279.

[1]V. Ambegaokar, P. G. de Gennes, and D. Rainer, Phys. Rev. A **9**, 2676 (1974).

[2]G. Barton and M. A. Moore, J. Low Temp. Phys. **21**, 489 (1975).

[3]L. H. Kjäldman, J. Kurkijärvi, and D. Rainer, J. Low Temp. Phys. **33**, 577 (1978).

[4]L. Buchholtz, Phys. Rev. B **33**, 1579 (1986).

[5]Nuclepore Corporation, 7035 Commerce Cir., Pleasanton, CA.

[6]J. M. Valles, Jr., D. T. Smith, and R. B. Hallock, Phys. Rev. Lett. **54**, 1528 (1985).

[7]M. T. Manninen and J. P. Pekola, Phys. Rev. Lett. **48**, 812 (1982), and J. Low Temp. Phys. **52**, 523 (1983).

[8]T. Chainer, Y. Morii, and H. Kojima, J. Low Temp. Phys. **55**, 353 (1984).

[9]The detectable pressure difference, P, across the membrane is given by $P=4\pi^2\Delta I f^2\theta/RA$, where ΔI is the detectable change in the moment of inertia, f the oscillator frequency, and θ the angular amplitude of oscillation. For θ of 10^{-8}, $\Delta I < 10^{-4} I(^3\mathrm{He})$, the consequent pressure resolution is better than 10^{-5} μbar.

[10]J. M. Parpia, D. G. Wildes, J. Saunders, E. K. Zeise, J. D. Reppy, and R. C. Richardson, J. Low Temp. Phys. **61**, 337 (1985).

[11]D. Vollhardt, K. Maki, and N. Schopohl, J. Low Temp. Phys. **39**, 79 (1980).

[12]J. P. Eisenstein, G. W. Swift, and R. E. Packard, Phys. Rev. Lett. **49**, 564 (1982).

[13]Ren-zhi Ling, D. S. Betts, and D. F. Brewer, Phys. Rev. Lett. **53**, 930 (1984); A. J. Dahm *et al.*, Phys. Rev. Lett. **45**, 1411 (1980).

[14]J. P. Pekola *et al.*, to be published.